Whole-System Assessment of the Benefits of Integrated Electricity and Heat System

Xi Zhang, *Student Member, IEEE*, Goran Strbac, *Member, IEEE*, Nilay Shah, Fei Teng, *Member, IEEE*, and Danny Pudjianto, *Member, IEEE*

***Abstract*—The interaction between electricity and heat systems will play an important role in facilitating the cost effective transition to a low carbon energy system with high penetration of renewable generation. This paper presents a novel integrated electricity and heat system model in which, for the first time, operation and investment timescales are considered while covering both the local district and national level infrastructures. This model is applied to optimize decarbonization strategies of the U.K. integrated electricity and heat system, while quantifying the benefits of the interactions across the whole multi-energy system and revealing the trade-offs between portfolios of: 1) low carbon generation technologies (renewable energy, nuclear, and CCS) and 2) district heating systems based on heat networks and distributed heating based on end-use heating technologies. Overall, the proposed modeling demonstrates that the integration of the heat and electricity system (when compared with the decoupled approach) can bring significant benefits by increasing the investment in the heating infrastructure in order to enhance the system flexibility that in turn can deliver larger cost savings in the electricity system, thus meeting the carbon target at a lower whole-system cost.**

***Index Terms*—Integrated energy system, combined heat and power (CHP), heat network, heat pump (HP), power system economics, renewable energy sources.**

NOMENCLATURE

Constants

α^{dsr}	Proportion of flexible electricity load that can provide DSR
$\alpha^{hp,res}$	Proportion of HPs output that can be interrupted to provide operating reserve service
α^{p}	Percentage of electricity demand supplied by representative distribution networks
α^{PH}	Proportion of heat load that can provide pre-heating
ε^{s}	Ratio of the energy capacity to power rating of TES
η^{PH}	Heat storage efficiency of pre-heating
η^{s}	Storage efficiency of TES
λ	Maximum ratio of heat to electricity for CHP
ς^{W}	Forecasting error of wind output
ς^{PV}	Forecasting error of PV output
ς^{D}	Forecasting error of electricity demand
τ	Total time horizon
a^{HP}/b^{HP}	Linear coefficient/constant term of COP for ASHP
a^{L}/b^{L}	Linear coefficient/constant term of LOLP function
$\overline{cap}^{DN}$	Peak electricity load that can be accommodated without network reinforcement
h	Heat demand
p	Electricity demand
$\underline{p}^{chp}$	Minimum electricity output of CHP units
$\overline{p}^{chp}$	Maximum electricity output of CHP units
$\underline{p}^{g}$	Minimum electricity output of generation units
$\overline{p}^{g}$	Maximum electricity output of generation units
r^{up}/r^{dn}	Ramp-up/ramp-down limit for generators
vre^{af}	Renewable energy availability factor
$\overline{rsp}^{g}$	Maximum response generation units can provide
z	Conversion rate from electricity to heat for CHP
AF	Annuity factor of different assets
C^{d}	Capital cost of various district heating assets
C^{e}	Capital cost of various end-use heating appliances
C^{f}	Capital cost of transmission networks
C^{g}	Capital cost of generators
C^{fix}	Fixed O&M cost of various assets
$C^{ins,e}$	Installation cost of end-use appliances
C^{DN}	Reinforcement cost of representative distribution networks
C^{DN}	Capital cost of heat networks per length
$\overline{Cap}^{L}$	Capacity of the largest generator
$\overline{CO2}$	Overall carbon target
COP^{a}	Coefficient of performance of air source HPs
COP^{w}	Coefficient of performance of water source HPs
$\overline{AAF}$	Annual availability factor of generators
$\overline{LOLE}$	Reliability criterion that sum of LOLP across the year should meet
OC^{gb}	Operation cost of various types of gas boilers
OC^{nl}	No-load cost of various generation
OC^{st}	Start-up cost of various types of generation
OC^{var}	Variable operation cost of various types of generation
N^{h}	Number of households

Manuscript received July 31, 2017; revised March 13, 2018, July 14, 2018, and September 14, 2018; accepted September 15, 2018. Date of publication September 27, 2018; date of current version December 19, 2018. This work was supported in part by the Engineering and Physical Sciences Research Council under Grant EP/K039326/1, and in part by the European Union's Horizon 2020 Research and Innovation Program (Project THERMOS) under Grant 723636. Paper no. TSG-01087-2017. *(Corresponding author: Xi Zhang.)*

The authors are with the Department of Electrical and Electronic Engineering, Imperial College London, London SW7 2AZ, U.K. (e-mail: x.zhang14@imperial.ac.uk).

Color versions of one or more of the figures in this paper are available online at http://ieeexplore.ieee.org.

Digital Object Identifier 10.1109/TSG.2018.2871559

N^{DN} Number of representative distribution networks
N^{HN} Number of representative heat networks
$\underline{OR}$ System operating reserve requirement
$\underline{FR}$ System frequency response requirement
T^a Ambient temperature.

Variables

μ Number of synchronized generation units
ω^d/ω^e Penetration of district /end-use heating technologies
ω^{HN} Penetration of HNs in each representative district
cap^x Capacity of plant/appliance x
cap^{DN} Expanded capacity of distribution networks due to reinforcement
h^{chp} Heat output of CHP
h^d/h^e Heat demand of district heating/end-use heating
h^{d+}/h^{d-} Increased/reduced heat demand due to pre-heating in district heating
h^{e+}/h^{e-} Increased/reduced heat demand due to pre-heating in end-use heating
h^{gb} Heat output of different types of gas boilers
h^{hp} Heat output of different types of HPs
h^{PH} Accumulated heat through pre-heating
p^{chp} Electricity output of CHP
p^{ele} Electricity load not related to heat
p^{ele+} Increased non-heat electricity demand through DSR
p^{ele-} Decreased non-heat electricity demand through DSR
p^{heat} Heat-driven electricity load
p^g Electricity output of generators
vre Output of variable renewable energy sources (VRE)
vre^{ava} VRE available for generation
vre^W Wind power output
vre^{PV} PV output
$res^{hp,e}$ Operating reserve provided by end-use HPs
res^x Operating reserve provision from source x
$rsp^{hp,e}$ Frequency response provided by end-use HPs
rsp^x Frequency response provision from source x
s^+/s^- Discharging/charging rate of different types of TES
s^{cap} Maximum discharging/charging rate of TES
s^{ec} Energy content of TES
$CO2$ Carbon emission from various sources
CM Capacity margin of generation
IC^{HN} Investment cost of representative HNs
$LOLP$ Estimated Loss of Load Probability.

Superscripts

chp CHP related
d District heating assets related
e End-use heating appliances related
f Transmission network related
g Generator related
gb Gas boiler related.

Functions

$F(\cdot)$ DC Power flow function
$F_L^{HN}(\cdot)$ Heat network length function
$F^{LOLP}(\cdot)$ LOLP function.

Sets

H_d/H_e Set of district/end-use heating technologies
D_x Set of time steps in the xth day (starting at midnight)
DN Set of representative distribution networks
HN Set of representative heat networks
DN_i Set of components included in distribution network i
F Set of transmission corridors
G Set of generation types
L Set of locations
T Set of operating time steps.

I. Introduction

HEATING accounts for approximately half of the total energy consumption and is responsible for over 25% of carbon emissions in the U.K. Therefore, decarbonization of the heat sector is one of the key challenges in achieving the 80% carbon reduction target by 2050 [1]. There is growing evidence that the interaction between electricity and heat systems will be important in facilitating cost effective transition to a lower carbon system by efficiently accommodating VRE. The lack of flexibility in the electricity system is a key limiting factor for effectively integrating VRE [2]–[4], whereas the heat system and the electrified transport sector can potentially provide considerable amount of flexibility by delivering a range of balancing services and support the management of peak demand [5]–[7]. Both district (HNs) and end-use heating technologies (e.g., end-use heat pumps) are potential options for the decarbonization of the heat sector. As presented in [6] and [8], HNs can alleviate wind curtailment through coordinated operation of CHP with thermal energy storage (TES). The potential role of HNs in a 100% renewable energy sources based energy system is investigated in [9]. CHP generation supplying heat to HNs is modeled in [6], [10], and [11], while the benefits of the application of industrial size HPs in HNs are outlined in [12]–[14]. In terms of end-use heating, the impacts of HPs on wind power integration have been investigated in [15] and [16] while [17]–[20] focuses on the analysis of hybrid heating technologies at consumer premises, which can potentially link electrical HPs, gas boilers and resistive heating devices. The economic and operational advantages of different combinations of end-use heating technologies are analyzed in [18] and [19], demonstrating the cost-effectiveness of hybrid electrical HPs and gas boilers (Hybrid HP-B). Integrated heat and electricity dispatch considering thermal inertia of buildings has been analyzed in [21]. HNs can also improve the efficiency of energy supply through pre-heating [22], [23]. TES, characterized with significantly lower capital cost than electricity storage, can further enhance the value of HNs in integrated electricity and heat

systems [24]. Similarly, benefits of end-use TES supporting hybrid HP-B are demonstrated in [18].

Previous research on the investment and operation optimization of HNs mostly focuses on the local level infrastructure [25]–[27]. Pudjianto *et al.* [28] proposed a whole-system investment model for the electricity system where HPs are assumed to be the only option for the decarbonization of the heat sector. In this context, a novel modeling framework for the whole system optimization of the combined electricity and heat system is proposed in this paper. In the context of the previous work, the proposed model for the first time considers operation and investment timescales while covering both local and national level of heat and electricity infrastructures. Furthermore, the impact of reduced system inertia on the frequency response requirements is explicitly modeled while security constraints and carbon emission targets are also included in the proposed framework. This approach is applied to optimize the decarbonization strategy of the combined electricity and heat system, selecting the cost effective portfolio of heating technologies, including HNs (supplied by CHP plants, industrial size HPs, gas boilers as well as TES), and consumer end hybrid HP-Bs. The proposed model simultaneously optimizes, for the first time, the investment in electricity generation (including conventional and low carbon generation), heating plants/appliances, HNs, reinforcement of electricity transmission and distribution networks while considering system operation cost and taking into account frequency regulation and operating reserve requirements.

Through several case studies, we demonstrate the interaction between electricity and heat systems across operation and investment timescale while simultaneously managing conflicts and synergies between local and national level objectives. Key contributions of this paper can be summarized as:

1) Presenting a novel combined electricity and heat system modeling framework considering both operation and investment timescales with spatial granularity including local and national level infrastructure.

2) Quantifying the benefits of the integrated planning of electricity and heat systems and demonstrating the impact on the technology mixes in both electricity and heat sectors.

II. Integrated Electricity and Heat System Model

A. Interactions Between Electricity and Heat Systems

As shown in Fig. 1, the electricity and heat systems are coupled through end-use hybrid HP-Bs as well as district based CHPs and HPs. The absence of coordination would drive inefficient investments in both electricity and heat systems (at both local and national level). On the other hand, inherent flexibility in the heat system can be used to alleviate these challenges through coordinated operation and investment with the electricity system. For instance, inherent storage in HN (the pipework) enhanced by TES and the CHP that adjusts power-to-heat ratio, can provide balancing service needed to support efficient integration of VRE, while reducing peak demand and the investment in back-up generation. Furthermore, if demand side response (DSR) is enabled, flexible end-use hybrid HP-Bs could bring benefits across all sectors of the electricity system. The developed model considers all these potential interactions so that the whole system benefits of the integrated electricity and heat system can be quantified.

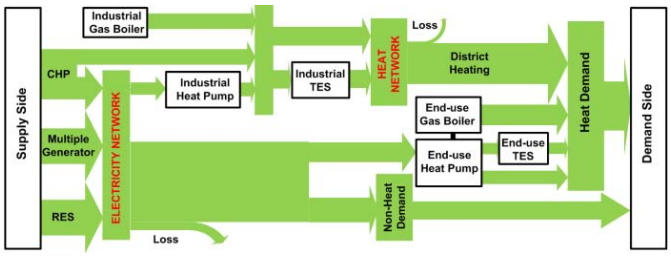

Fig. 1. Interaction and energy balance of integrated electricity and heat system.

B. Model of Integrated Electricity and Heat System Investment

This model is formulated as a mixed integer linear programming problem with hourly time resolution across a whole year, while also considering sub-hourly frequency regulation and reserve constraints. The objective function (1) is to minimize the whole system cost which includes the annual operation costs and the annuitized investment costs related to different types of generation, heating plants/appliances, energy storage as well as electricity and heat networks:

The annual system operation costs include fuel costs of generators, CHPs and gas boilers. The operation costs of generators/CHPs consist of (i) variable cost which is associated with the generation output, (ii) no-load cost which is determined by the number of synchronized units and (iii) start-up cost. These operation cost categories are modeled based on the piecewise linear approximation approach proposed in [29]; Gas boilers serve as supplementary heating devices that are used to reduce the capacity of electrification-based heating plants/appliances (e.g., CHPs and HPs) and electricity infrastructure reinforcement. In this model, both industrial size gas boilers (applied in district heating) and end-use gas boilers (working as a part of hybrid HP-Bs) are taken into consideration. Carbon price is included in the fuel cost.

The annuitized infrastructure investment costs include capital costs of generators, district heating assets (superscripted by d, including HNs, CHPs, industrial size HPs, industrial size TESs and industrial size gas boilers), end-use heating appliances (superscripted by e, including hybrid HP-Bs and end-use TESs), and reinforcement costs of transmission and distribution networks. Annuity factors for different assets are considered given corresponding discount rates and life spans.

$$Min\ \varphi = \sum_{t=1}^{T}\sum_{i=1}^{G}\sum_{j=1}^{L}\Big(p_{t,i,j}^{g}\cdot OC_i^{var} + \mu_{t,i,j}\cdot OC_i^{nl} + \mu_{t,i,j}^{st}\cdot OC_i^{st}\Big) + \sum_{t=1}^{T}\sum_{j=1}^{L} h_{t,j}^{gb,d}\cdot OC^{gb,d} + \sum_{t=1}^{T}\sum_{j=1}^{L} h_{t,j}^{gb,e}\cdot OC^{gb,e}$$

$$
\begin{aligned}
&+\sum_{i=1}^{G}\sum_{j=1}^{L}\left(C_i^g \cdot AF_i^g + C_i^{fix,g}\right)\cdot cap_{i,j}^g \\
&+\sum_{i=1}^{F} C^f \cdot AF_i^f \cdot cap_i^f \\
&+\sum_{i=1}^{H_d}\sum_{j=1}^{L}\left(C_i^d \cdot AF_i^d + C_i^{fix,d}\right)\cdot cap_{i,j}^d \\
&+\sum_{i=1}^{H_e}\sum_{j=1}^{L}\Big(\left(C_i^e \cdot AF_i^e + C_i^{fix,e}\right)\cdot cap_{i,j}^e \\
&\qquad + N_j^h \cdot \omega_j^e \cdot C_i^{ins,e} \cdot AF_i^e\Big) \\
&+\sum_{i=1}^{DN} C_i^{DN} \cdot cap_i^{DN} + \sum_{i=1}^{HN} \omega_i^{HN} \cdot N_i^{HN} \cdot IC_i^{HN} \qquad (1)
\end{aligned}
$$

This model takes account of a variety of operation constraints while minimizing the whole system cost as well as meeting the carbon target. All these constraints are applied on hourly time resolution ($\forall t \in T$) across all locations ($\forall j \in L$), which include:

1) Electricity Balance Constraints: Constraint (2) ensures that electricity supply and demand are balanced in each time interval within the entire electricity system. Electricity demand consists of non-heat based demand (that may be redistributed through DSR) and heat-driven electricity demand (particularly referring to the demand of end-use HPs and industrial size HPs), as shown in (3-4). In this modeling, air source HPs (ASHP) are applied for end-use heating. For district heating systems, water source HPs (WSHP) are applied due to their high efficiency. As the ambient temperature varies significantly, the COP of ASHPs will change accordingly (5). On the other hand, the COP of WSHPs is assumed to be constant given that the water source temperature tends to be stable.

$$\sum_{i=1}^{G}\sum_{j=1}^{L} p_{t,i,j}^g = \sum_{j=1}^{L} p_{t,j} \qquad (2)$$

$$p_{t,j} = \left(p_{t,j}^{ele} + p_{t,j}^{ele+} - p_{t,j}^{ele-}\right) + p_{t,j}^{heat} \qquad (3)$$

$$p_{t,j}^{heat} = h_{t,j}^{hp,e}/COP_t^a + h_{t,j}^{hp,d}/COP^w \qquad (4)$$

$$COP_t^a = a^{HP} \cdot T_t^a + b^{HP}. \qquad (5)$$

2) Heat Balance Constraints: Constraint (6) shows the energy balance for the heat system. On the supply side, both district and end-use heating systems are considered. District heating system is supplied by CHPs, industrial size HPs, gas boilers and TESs, as shown in (7), while end-use heating appliances includes end-use hybrid HP-Bs and TESs, as presented in (8).

$$\sum_{i=1}^{H_d} h_{t,i,j}^d - h_{t,j}^{d+} + h_{t,j}^{d-} + \sum_{i=1}^{H_e} h_{t,i,j}^e - h_{t,j}^{e+} + h_{t,j}^{e-} = h_{t,j} \qquad (6)$$

$$\sum_{i=1}^{H_d} h_{t,i,j}^d = h_{t,j}^{chp} + h_{t,j}^{hp,d} + h_{t,j}^{gb,d} + s_{t,j}^{+,d} - s_{t,j}^{-,d} \qquad (7)$$

$$\sum_{i=1}^{H_e} h_{t,i,j}^e = h_{t,j}^{hp,e} + h_{t,j}^{gb,e} + s_{t,j}^{+,e} - s_{t,j}^{-,e}. \qquad (8)$$

3) Heating Technology Mix Constraints: The overall heat demand is supplied by both district heating technologies and end-use heating technologies as stated in (9) and (10), while ensuring that all heat demand is satisfied (11):

$$\sum_{i=1}^{H_d} h_{t,i,j}^d - h_{t,j}^{d+} + h_{t,j}^{d-} = \omega_j^d \cdot h_{t,j} \qquad (9)$$

$$\sum_{i=1}^{H_e} h_{t,i,j}^e - h_{t,j}^{e+} + h_{t,j}^{e-} = \omega_j^e \cdot h_{t,j} \qquad (10)$$

$$\omega_j^d + \omega_j^e = 1. \qquad (11)$$

4) Power Flow Constraint: In this modeling, DCOPF is performed to optimize the capacity and the location of reinforcement of transmission networks. Constraint (12) is applied for all transmission lines ($\forall m \in F$), where G, D and θ represent electricity generation, electricity demand and voltage angle at each location:

$$-cap_m^f \le F(G, D, \theta)_{t,m} \le cap_m^f. \qquad (12)$$

5) DSR Constraints: The flexibility provided by flexible electricity load and ancillary service provision through short term interruption of operation of end-use HPs are included in the model. Based on the DSR model presented in [28], (13) limits the amount of shiftable load (particularly referring to electrical vehicles and smart appliances, e.g., smart dishwasher and fridge, which have broad consumer acceptance of DSR). Note that α^{dsr} depends on the consumers' willingness to shift load which can change with time. For simplicity, we assumed that it is not time-dependent. Constraint (14) gives the demand balance of DSR (in this case study it is assumed that most of the residential flexible demand can be shifted within a day). The contribution of end-use HPs in providing ancillary services is shown in (15) and (16).

$$p_{t,j}^{ele-} \le \alpha^{dsr} \cdot p_{t,j}^{ele} \qquad (13)$$

$$\sum_{t\in D_x} p_{t,j}^{ele-} \le \sum_{t\in D_x} p_{t,j}^{ele+} \qquad (14)$$

$$rsp_{t,j}^{hp,e} \le h_{t,j}^{hp,e}/COP_t^a \qquad (15)$$

$$res_{t,j}^{hp,e} \le \alpha_j^{hp,res} \cdot h_{t,j}^{hp,e}/COP_t^a. \qquad (16)$$

6) TES Operating Constraints: In this model, TES specifically refers to the hot water tank. The maximum discharging and charging rate is restricted by (17) (it is assumed that the maximum discharging rate is equal to the maximum charging rate). Energy capacity is limited by (18) where ε^s is the ratio of the energy capacity to the power rating of TES. The energy balance constraint is presented as (19). Constraints (17)-(19) are applied for both industrial size TES and end-use TES.

$$s_{t,j}^{+} \le s_j^{cap},\ \ s_{t,j}^{-} \le s_j^{cap} \qquad (17)$$

$$s_{t,j}^{ec} \le s_j^{cap} \cdot \varepsilon^s \qquad (18)$$

$$s_{t,j}^{ec} = s_{t-1}^{ec} \cdot \eta^s + s_{t,j}^{-} - s_{t,j}^{+}. \qquad (19)$$

7) Pre-Heating Constraints: Pre-heating can be applied in both district heating (through the inherent storage in HN pipelines [22]) and end-use heating systems (through the thermal insulation of buildings). Constraints (20)-(22) present a generic pre-heating model for both district and end-use heating systems. Constraint (20) presents the amount of heat demand that can be shifted, which depends on the flexibility of heat systems. In district heating systems, the flexibility is driven by the capacity of the inherent storage of HN pipelines as the proportion of heat demand can be redistributed ($\alpha^{PH,d}$). It is worth noticing that the storable energy in HN pipelines is typically limited (one or two hours' worth of heat content) due to the constant flow of heat in the pipelines. In end-use heating systems, the flexibility is measured by the percentage of residential buildings ($\alpha^{PH,e}$) that have the potential to participate in pre-heating (with good insulation and a large mass of envelope which can provide a meaningful amount of storage). Constraint (21) ensures that the increased load for pre-heating is limited by the capacity of the heating devices. The energy balancing process of pre-heating is simplified as a storage model (22). In this modeling it is assumed that the average heat loss rate is proportional to the stored heat. The uncertainty related to pre-heating heat losses is further investigated through sensitivity studies presented in Section IV.

$$h^{x-}_{t,j} \le \alpha^{PH,x} \cdot \sum_{i=1}^{H_x} h^{x}_{t,i,j} \ , \ x \in \{d, e\} \tag{20}$$

$$h^{x+}_{t,j} \le \alpha^{PH,x} \cdot \sum_{i=1}^{H_x} cap^{x}_{i,j} \ , \ x \in \{d, e\} \tag{21}$$

$$h^{PH,x}_{t,j} = h^{PH,x}_{t-1} \cdot \eta^{PH,x} + h^{x+}_{t,j} - h^{x-}_{t,j} \ , \ x \in \{d, e\}. \tag{22}$$

8) Generation Unit Constraints: These constraints incorporate minimum stable generation and maximum output (23); ramp-up (24) and ramp-down constraint (25); start-up constraints (26)-(27); the availability of ancillary service (28); maximum reserve and response provided by each generation technology (29-30); annual energy production of generation limits associated with scheduled inspection and maintenance (31); and the total capacity of different generation technologies (32).

$$\mu_{t,i,j} \cdot \underline{p}^{g}_{j} \le p^{g}_{t,i,j} \le \mu_{t,i,j} \cdot \overline{p}^{g}_{j} \tag{23}$$

$$p^{g}_{t,i,j} - p^{g}_{t-1,i,j} \le \mu_{t,i,j} \cdot r^{up}_{i} \tag{24}$$

$$p^{g}_{t-1,i,j} - p^{g}_{t,i,j} \le \mu_{t,i,j} \cdot r^{dn}_{i} \tag{25}$$

$$\mu^{st}_{t,i,j} \ge \mu_{t,i,j} - \mu_{t-1,i,j} \tag{26}$$

$$\mu^{st}_{t,i,j} \ge 0 \tag{27}$$

$$\mu_{t,i,j} \cdot \underline{p}^{g}_{j} \le p^{g}_{t,i,j} + rsp^{g}_{t,i,j} + res^{g}_{t,i,j} \le \mu_{t,i,j} \cdot \overline{p}^{g}_{j} \tag{28}$$

$$res^{g}_{t,i,j} \le \mu_{t,i,j} \cdot \overline{res}^{g}_{i,j} \tag{29}$$

$$rsp^{g}_{t,i,j} \le \mu_{t,i,j} \cdot \overline{rsp}^{g}_{i,j} \tag{30}$$

$$\sum_{t=1}^{T} p^{g}_{t,i,j} \le \overline{AAF}_{i} \cdot \tau \cdot cap^{g}_{i,j} \tag{31}$$

$$\mu_{t,i,j} \cdot \overline{p}^{g}_{j} \le cap^{g}_{i,j}. \tag{32}$$

9) VRE Curtailment: The curtailment of VRE is the difference between available VRE power (vre^{ava}) in (33) and the actual output of VRE (vre) in (34).

$$vre^{ava}_{t,i,j} = vre^{af}_{t,i,j} \cdot cap^{g}_{i,j} \ , \ i \in \{wind, solar\} \tag{33}$$

$$vre_{t,i,j} \le vre^{ava}_{t,i,j} \ , \ i \in \{wind, solar\}. \tag{34}$$

10) Ancillary Service Constraints: Two key categories of balancing services are considered in this model, including frequency response which is scheduled to tackle the sudden generation outage of the electricity system and operating reserve driven by the forecasting errors of renewables and load and the replacement of primary response. The frequency response constraint and operating reserve constraint are formulated as (35) and (36), respectively. It should be noted that (35) also ensures that adequate amount of synchronous generation is scheduled to operate in order to provide sufficient level of inertia. The frequency response requirement is directly linked with the level of system inertia (which can be seen as linear to the online synchromous capacity) in each time interval, which is critical in the future low inertia system. This requirement is derived based on the work presented in [30]. A complete MILP formulation was proposed in [31], which used a piecewise linear version of the constraint (as shown in Fig. 2) to reduce the computational burden of the proposed large-scale model. Operating reserve requirements are determined by forecasting errors of wind output, PV output, electricity load and the capacity of the largest generator to cover the worst case, as formulated in (37). Note that in this model, the actual utilization of reserve and response services is not explicitly modeled. This would require a two-stage model considering generation and demand realizations, which would substantially increase the complexity of the analysis. Similar simplifications have been commonly made in the development of whole-system energy models (e.g., [8] and [28]). Hence technologies in district heating (through CHPs and HPs) as well as end-use heating systems could provide ancillary services for the electricity system based on these constraints:

$$\sum_{i=1}^{G}\sum_{j=1}^{L} rsp^{g}_{t,i,j} + \sum_{i=1}^{H_d}\sum_{j=1}^{L} rsp^{d}_{t,i,j} + \sum_{i=1}^{H_e}\sum_{j=1}^{L} rsp^{e}_{t,i,j} \ge \underline{FR}_{t} \tag{35}$$

$$\sum_{i=1}^{G}\sum_{j=1}^{L} res^{g}_{t,i,j} + \sum_{i=1}^{H_d}\sum_{j=1}^{L} res^{d}_{t,i,j} + \sum_{i=1}^{H_e}\sum_{j=1}^{L} res^{e}_{t,i,j} \ge \underline{OR}_{t} \tag{36}$$

$$\underline{OR}_{t} = \varsigma^{W} \cdot vre^{W}_{t} + \varsigma^{PV} \cdot vre^{PV}_{t} + \varsigma^{D} \cdot p_{t} + Cap^{L}. \tag{37}$$

11) CHP Operating Constraints: The operating area of CHP is illustrated in Fig. 3, which is modeled by (38-39). CHP can change its heat and electricity ratio by adjusting the amount of steam extracted from the turbine, the slope of the upper bound (equal to $-1/z$) gives the ratio of the change of electricity output to the corresponding change of heat output. For a given fuel feeding rate, if the steam extraction changes, operating points will move along the lines which are parallel with the upper bound. For any point (A) within the operating area, there is a corresponding point (A') on the y-axis which is characterized by the same fuel feeding rate as A ($\overline{AA'}$ is parallel with the upper bound) [11]. In order to apply the generation

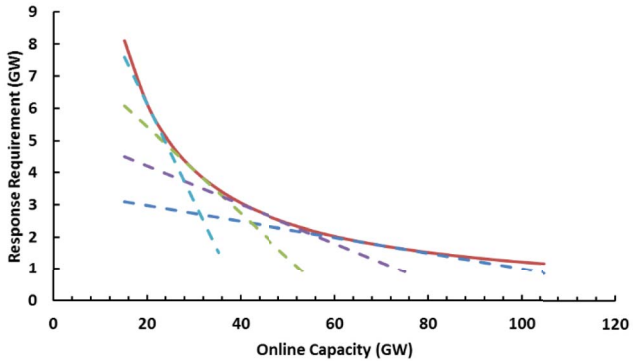

Fig. 2. Piecewise linear function of frequency requirement of the system.

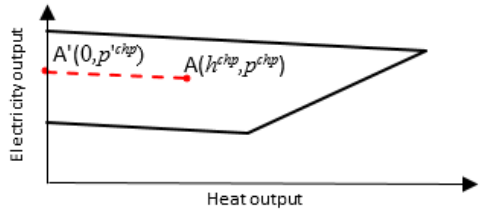

Fig. 3. Operating area of CHP.

model which is formulated in (23-32) to CHP, all the operating points of CHP are converted into the corresponding points on the y-axis (electricity-only mode), as shown in (40).

$$\mu_{t,i,j} \cdot \underline{p}_j^{chp} \le p_{t,j}^{chp} + h_{t,j}^{chp}/z_j \le \mu_{t,i,j} \cdot \overline{p}_j^{chp} \tag{38}$$

$$h_{t,j}^{chp} \le \lambda_j \cdot p_{t,j}^{chp} \tag{39}$$

$$p_{t,i=CHP,j}^{g} = p'^{chp}_{t,j} = p_{t,j}^{chp} + h_{t,j}^{chp}/z. \tag{40}$$

12) Distribution Network Reinforcement Constraint: Based on the distribution network reinforcement model presented in [28], the cost of reinforcing distribution networks is formulated as a function of the expanded capacity of the distribution network (cap^{DN}). A schematic function of the distribution network reinforcement cost has been illustrated in [28], while a linear approximation of this function is applied in this paper as formulated in (1). cap^{DN} is determined by the net increase of peak demand within the distribution network, as shown in (41).

$$-cap_i^{DN} \le \alpha_i^p \cdot p_t - \sum_{j \in DN_i} p_{t,j}^g - \overline{cap}_i^{DN} \le cap_i^{DN}, \forall i \in DN \tag{41}$$

It is assumed that CHP and PV are deployed in the distribution network. The cost coefficient (C^{DN} in the objective function) is derived through the analysis of the network reinforcement cost driven by the increase in peak demand by applying the fractal-based algorithm proposed by [32]. The created representative distribution networks based on this algorithm have been calibrated by the analysis of the corresponding real distribution networks. Although the parameters of real networks are very case-specific and vary significantly, the analysis of the large regions characterised by the representative networks provides an estimate of the real network reinforcement cost. As described in [33], key typical representative distribution networks, covering urban, sub-urban, semi-rural, or rural areas, are created by using the fractal-based algorithm and are incorporated into this model.

13) Heat Network Investment Cost: As the key indicator of HN investment cost, heat density is used to compartmentalize Great Britain (GB) into different district types covering urban, suburban, semirural and rural areas. By using the fractal-based algorithm proposed in [32], generic heat networks are created covering representative districts with different heat densities. The number of consumers and heat demand in representative districts are obtained from the National Heat Map [34] and applied as inputs into the fractal-based algorithm to establish the topologies and further calculate the length of the representative heat networks which drives their investment costs. Equation (42) determines the capital cost of representative HNs, where C_i^{DN} denotes the capital cost (per length) of HNs while $F_L^{HN}(\cdot)$ calculates the length of representative HNs based on the fractal-based algorithm, given the size of area, number of consumers and heat demand in the representative districts. Table VI demonstrates the length of different representative HNs.

By applying the approach proposed in [33] and [35], the whole GB area is represented by a combination of different types of representative districts, while minimizing the errors of the total heat demand, the number of households and the size of geographical areas between the calculated data and the realistic data. The number of different representative HNs, denoted as N^{HN} in (1), has been optimized exogenously, as given in Table VI. By applying this concept, the investment cost associated with different penetrations of HN (ω^{HN} in (1)) in each representative district can be quantified and then incorporated into the whole system investment model to optimize the share of HN.

$$IC_i^{HN} = C_i^{DN} \cdot F_L^{HN}\left(A_i, N_i^h, \sum_{t \in T} h_{t,j}\right), \forall i \in HN. \tag{42}$$

14) Security Constraints: Constraint (43) ensures that the model will propose a sufficient generating capacity to achieve a given level of security specified by LOLE. To achieve this, LOLP is estimated as a function of the capacity margin (which is defined as the ratio of the surplus generating capacity to the peak demand, as formulated in (44)) and is built exogenously through the standard reliability approach by applying generation availability data [28]. The piecewise linear approximation of the LOLP function presented in [28] is applied in this paper, as shown in (45).

$$\sum_{t=1}^{T} F^{LOLP}(CM_t) \le \overline{LOLE} \tag{43}$$

$$CM_t = \frac{\sum_{i=1}^{G}\sum_{j=1}^{L}\left(\mu_{t,i,j} \cdot \overline{p}_j^g - p_j^g\right)}{\max_{t \in T}\left(\sum_{j=1}^{L} p_{t,j}\right)} \tag{44}$$

$$F^{LOLP}(CM_t) \ge a_1^L \cdot CM_t + b_1^L$$
$$\vdots$$
$$F^{LOLP}(CM_t) \ge a_n^L \cdot CM_t + b_n^L. \tag{45}$$

15) Carbon Constraint: Constraint (46) ensures that the total carbon emissions do not exceed the regulated amount of carbon emissions, which is defined as the product of the given overall carbon target ($\overline{CO2}$) and the annual energy consumption, covering both electricity and heat sectors.

$$\sum_{t=1}^{T}\sum_{i=1}^{G}\sum_{j=1}^{L} CO2^{g}_{t,i,j} + \sum_{t=1}^{T}\sum_{j=1}^{L} CO2^{gb}_{t,j} \leq \overline{CO2} \cdot \sum_{t=1}^{T}\sum_{j=1}^{L}\left(h_{t,j} + p^{heat}_{t,j}\right). \quad (46)$$

III. Case Study: 2030 GB System

A. System Description

The integrated electricity and heat system model proposed in Section III is applied to two GB 2030 scenarios, with different carbon targets, involving different mixes of low carbon generation: (a) 100g/kWh, (50GW wind, 20GW PV and 8GW nuclear) and (b) 50g/kWh, (80GW wind, 35GW PV and 10GW nuclear). In both scenarios, natural gas (NG) based CCS plants are allowed to be added to the mix if the carbon targets cannot otherwise be satisfied. In the integrated electricity and heat system, the overall carbon emissions are quantified from all sources involved in meeting both electrical and thermal demand.

Regarding decarbonization of heat sector it is assumed that HNs and hybrid HP-Bs are two main technologies delivering low-carbon heat in 2030. The pattern of heat demand is based on [1], with peak demand estimated at 247GW and annual thermal energy demand at 370TWh. It is assumed that 77% of annual heat demand is for space heating while 23% for water heating [18]. The electricity demand is divided into non-heat electricity demand and heat-driven electricity demand. The maximum non-heat electricity demand is estimated at 72GW while the minimum demand at 19GW, with annual energy of 325TWh. The heat-driven electricity demand depends on the optimized electrification rate of heat demand.

The GB transmission system is characterized by significant North to South power flows and represented by 5 regions, including 1) Scotland, 2) North England and Wales, 3) Middle England and Wales, 4) South England and Wales and 5) London (embedded in South England and Wales). Fig. 4 illustrates the topology of the simplified network together with the length and existing capacity of the transmission corridors connecting the key regions. In each of the regions, appropriate combinations of different district network types represent HNs and electricity distribution networks, following the approach proposed in [33].

Cost and operation data for different types of generation are listed in Table I [36], Table II [3], [36] and Table III [3], while the data for heating technologies are given in Table IV [18], [37]. The capital cost of heating technologies is nnualized by a discount rate of 10% and a lifespan of 20 years. As gas boilers have already been installed in most residential houses in the U.K., we assume that the deployment of hybrid HP-B does not incur investment cost of gas boilers. On the other hand, the cost of the smart control device that is required to optimize the operation of hybrid HP-B between ASHPs and gas boilers is considered in this model (80£/household according to [18]). The capital cost of ASHP applied in this paper is based on small-size ASHP. A fixed instalation cost is considered for any size of ASHP. Based on [37], the

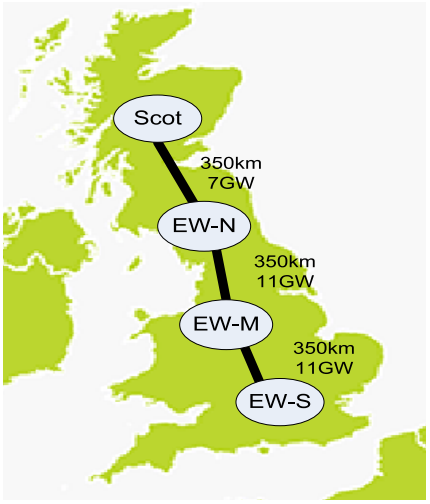

Fig. 4. Schematic topology and the existing capacity of the GB transmission links between the key regions.

TABLE I
Cost Parameters of Generation Plants

Generation	Capital cost (£m/MW)	Fixed O&M (£/kW/year)	Variable O&M (£/MWh)	Discount Rate	Lifetime (year)
Nuclear	4.34	83.4	5	8.90%	60
CCGT	0.51	16.6	3	7.80%	25
OCGT	0.32	8.2	3	7.80%	25
NG CCS	2.15	41.6	3	9.20%	25
Coal CCS	2.43	92.7	3	8.20%	15
NG CHP	0.76	34.4	5	7.80%	25
Biomass CHP	5.17	304.7	11	12.20%	24
Wind	1.52	30.9	5	8.90%	23
PV	0.67	6.2	0	6.50%	25

TABLE II
Operation Parameters of Generation Plants

Generation	Min stable generation	Ramp rates	Annual Availability Factor	Max Response provision	Max Reserve provision
Nuclear	80%	10%	0.91	0%	0%
CCGT	50%	60%	0.93	10%	50%
OCGT	40%	100%	0.93	10%	60%
NG CCS	50%	50%	0.93	10%	50%
Coal CCS	40%	50%	0.93	5%	60%
NG CHP	50%	60%	0.93	10%	50%
Biomass CHP	50%	60%	0.93	10%	50%
Wind	N/A	N/A	0.39	0%	0%
PV	N/A	N/A	0.12	0%	0%

TABLE III
CARBON AND OPERATING COST PARAMETERS OF THERMAL GENERATORS

Generation technology	Average cost (£/kWh)		Efficiency		Average CO2 emissions (g/kWh)	
	MSG	Full	MSG	Full	MSG	Full
Coal CCS	54.4	39.5	25.4%	35.0%	116	80
CCGT	84.7	74.1	51.5%	58.8%	422	368
CCGT CCS	63.4	55.9	45.2%	51.3%	39	34
OCGT	139.7	124.5	31.2%	35.0%	689	613
NG CHP	84.7	74.1	51.5%	58.8%	422	368
Biomass CHP	42.9	37.5	34.8%	39.8%	0	0

TABLE IV
COST PARAMETERS OF HEATING TECHNOLOGIES IN 2030

End-use heating	Capital cost (£/kW$_{th}$)	Installation (£)	O&M fixed (£/kW$_{th}$ /yr)	Efficiency (%)
ASHP	612	1200	20	1.6-3.6
Gas boiler	N/A	N/A	32	95%
District heating	Capital cost (£m/MW$_{th}$)		O&M fixed (£/MW$_{th}$/yr)	Efficiency (%)
HP	0.48		3200	380%
Gas boiler	0.08		2960	98%

TABLE V
PARAMETERS OF DISTRIBUTION NETWORKS IN 2030

	Percentage of demand supplied	Unit Reinforcement cost (£/kVA/year)	Peak load that can be accommodated without reinforcement (GW)
Urban	33.3%	37	5
Suburban	41.2%	62	4.8
Semirural	17.8%	26	2.1
Rural	7.7%	19	1

capital costs of end-use TES and industrial size TES are estimated at 2.4£/litre and 80£/m^3 (with installation and O&M costs included), with the same stationary loss rate of 1% per hour. It is also assumed that the ratio of the energy capacity to the power rating of TES (ε^s) is 3 hours for end-use TES and 6 hours for industrial TES. Relative parameters of representative distribution networks and heat networks are estimated in Table V [33] and Table VI [38]. The annual heat loss in HN is assumed at approximately 5% of the total heat distribution based on [39]. It should be stressed that different results can be obtained based on different cost assumptions, but the model can be applied in different scenarios.

This model is implemented by using FICO Xpress as a solver on a computer with two 2.7GHz processors and 512GB RAM (Intel Xeon CPU E5-2697 v2 @ 2.70GHz 2.70 GHz (2 processors) 512 GB RAM). It takes 3.19×10^5 s to solve the integrated case in Section III-B under the carbon target of 50g/kWh. As running the proposed model over a whole year with hourly resolution is very time-consuming, it is common to use a set of representative days to simulate the whole year (e.g., [40]–[42]).

TABLE VI
CAPITAL COST OF HEAT NETWORKS

Type of areas	Capital cost of HN (£/km)	Network length of representative HN (km)	Number of representative HN
Urban	1122	16.8	3632
Suburban	772	12.9	4536
Semirural	597	20.4	7300
Rural	468	39.6	5992

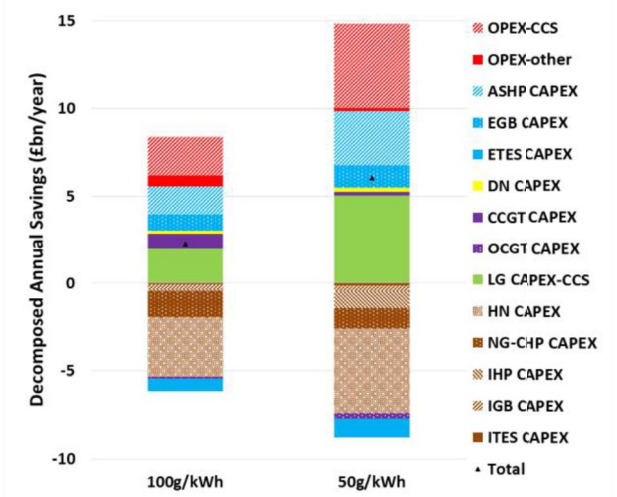

Fig. 5. Savings from the integration of electricity and heat systems.

B. Overall Benefits of Integrated Electricity and Heat System

In order to quantify the benefits through the integration of electricity and heat systems, the whole system costs of the integrated and decoupled systems are compared. Fig. 5 presents the annual savings in different system segments enabled by the integration of electricity and heat systems in two carbon scenarios considered.

As shown in Fig. 5, the integration of electricity and heat systems delivers significant savings in operation costs (OPEX), represented by red blocks, comprising operation costs of NG CCS, NG CHP, CCGT, OCGT and gas boilers, driven by significantly enhanced flexibility and efficiency of system operation through application of more efficient CHP and reduced renewable curtailment; Blue blocks indicate savings in capital costs (CAPEX) related to end-use heating technologies, including ASHP, end-use gas boilers (EGB), as a proportion of heat demand is supplied by HNs; Relatively minor investment savings are achieved in reducing capital expenditure associated with conventional generation (including CCGT and OCGT) and distribution networks (DN), as change in peak demand is not significant given that end-use heating is supplied by hybrid HPs (i.e., gas boilers are used to supply heat demand during peaks). Significant system integration driven savings are made by reducing the capacity of low-carbon generation (LG CAPEX), particularly referring to NG CCS (shown in green), as renewable generation is curtailed much

less (particularly in 50g/kWh carbon scenario), so the carbon targets can be met by reducing NG CCS capacity. Brown blocks present additional integration driven capital expenditure (negative savings) in district heating, including heat network pipelines (HN), NG CHP plants, industrial heat pumps (IHP), industrial gas boilers (IGB), and industrial thermal energy storage (ITES). Additional investment in end-use thermal energy storage (ETES) is also driven by the system integration.

The total annual saving through the system integration (denoted as "Total") is influenced by the carbon target. Fig. 5 shows that the annual saving is about £2.3bn/year (3.53% of the total annual system cost of the decoupled system) under the overall carbon target of 100g/kWh while the saving increases to £6bn/year (8.69% of the total annual system cost of the decoupled system) under the overall carbon target of 50g/kWh. Further simulations have been performed to investigate the relationship between the annual saving through the system integration and the intensity of the carbon target. When the carbon constraint is above 266g/kWh, the total system cost of both integrated and decoupled case is no longer influenced by the carbon constraint.

Fundamentally, the benefits of the integrated investment planning come from the flexibility that the heat system provides to the electricity system, which significantly reduces both investment and operation costs of the electricity system, while increasing investment in the heat system. To be more specific, CHP, industrial size HPs and thermal energy storage, typically deployed in heat networks, can provide ancillary services for the electricity system. End-use heat pumps, through temporarily turning down their output (which will not compromise the comfort due to the thermal inertia of buildings), can also provide ancillary services. Moreover, preheating can further enhance the flexibility of the electricity system. In the planning stage, if we consider the flexibility which heat systems can potentially provide for the electricity systems, significant savings can be achieved in the electricity side on the cost of increasing the investment on the heat side, but the overall system costs are reduced significantly. If the heat system and electricity system are planned separately, the requirement of flexibility in the electricity system has to be met by the components within the electricity system, incurring dramatic flexibility associated cost, which will otherwise incur little extra costs with the flexibility provision from the heat systems.

C. Impact of Integration on Electricity System

Fig. 6 presents the generation mix and annual electricity production in different scenarios. It is important to note that the total amount of generation capacity is very similar in integrated and decoupled scenarios (as peak demands are broadly the same in both scenarios). We can also observe that the reduction in CCGT and NG CCS capacity, which is driven by the enhanced flexibility and reduced VRE curtailment (as presented in Fig. 6 (b) and Table VII) through the system integration, requires increase in firm generation capacity to meet the security supply, which is achieved by NG CHP and OCGT plant. It is worth stressing that the model selects the economically optimal portfolio of electricity generation. In other

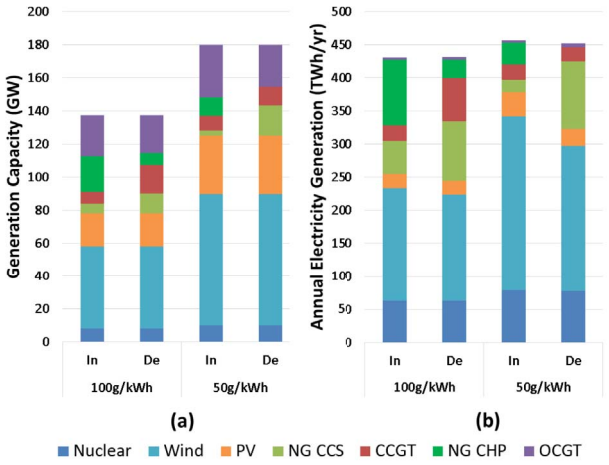

Fig. 6. (a) Generation mix and (b) annual electricity generation of integrated and decoupled cases under different carbon scenarios.

TABLE VII
ANNUAL CURTAILMENT OF VRE IN DIFFERENT SCENARIOS

Carbon target (g/kWh)	System	Wind curtailment (TWh/year)	Solar curtailment (TWh/year)
100	Integrated	0.62	0.00
	Decoupled	10.55	0.05
50	Integrated	10.07	1.13
	Decoupled	53.72	10.42

words, given the cost assumptions, large-scale deployment of other types of generation (e.g., biogas-based, biomass-based, etc.) is not seen to be economic compared to the generation types selected by the model, from the whole-system point of view.

The case study illustrated in Fig. 6 is performed under the given GB 2030 scenarios proposed by the U.K. government with fixed amount of nuclear, wind and PV (as described in Section III-A). If the carbon targets cannot be met by the given amount of low-carbon generation, additional NG CCS would be added to deliver the carbon target. Fig. 6 demonstrates the impact of the system integration on the curtailment of VRE. Due to the lack of flexibility in the decoupled system, significant amount of VRE is curtailed, and hence additional capacity of NG CCS is required to deliver the carbon target, which significantly increases the cost. To further reveal the impact of system integration on the overall electricity generation mix, we perform the case study (presented in Fig. 7) in which the capacities of all types of low carbon generation are optimized while meeting the same carbon targets. Instead of demonstrating the impact of the system integration on the curtailment of VRE, Fig. 7 focuses on the optimal generation portfolios.

It can be observed in Fig. 7 that considerable capacity of wind and PV generation is installed in the integrated system while in the decoupled scenarios more nuclear and NG CCS is required due to the inability of the system to effectively utilize VRE. This is because the additional costs that are incurred due to the integration of VRE can be significantly reduced by the increased flexibility provided by the integration

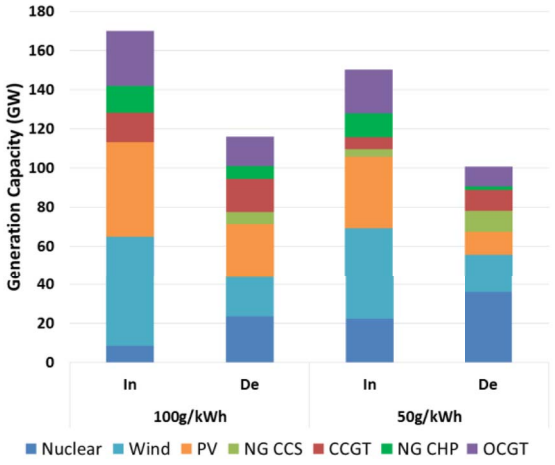

Fig. 7. Cost optimal generation mix for different scenarios.

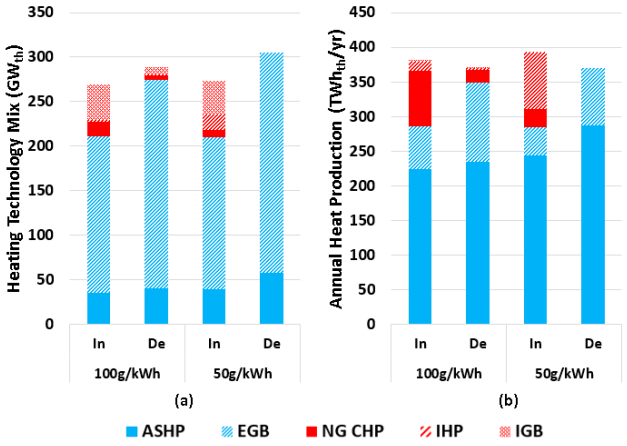

Fig. 8. (a) Heating technology mix and (b) annual heat production of integrated and decoupled cases under different carbon scenarios.

TABLE VIII
PENETRATION OF HNS IN URBAN AREA

Carbon target (g/kWh)	System	Penetration of HNs in urban areas (%)
100	Integrated	61.4%
	Decoupled	15.4%
50	Integrated	64.0%
	Decoupled	0%

of the electricity and heat system. This case study indicates that coupling the energy sectors can significantly increase the utilization of VRE.

It is important to emphasis that we assume VRE cannot provide frequency response in this paper, although our previous work [43] has clearly shown the potential value of VRE providing inertia and frequency response for the electricity system. However, on the technology side, the measurement of rate of change of frequency and coordination among large number of wind turbines still need to be resolved. On the economy side, the recovery effect of inertia provision and curtailment of VRE for frequency response provision may prevent its large-scale deployment. Of course, with the technology development, all these issues may be resolved and VRE can efficiently provide inertia and frequency response, leading to less benefits from energy system integration.

D. Impact of Integration on Heat System

The heating technology mix and annual thermal energy production in different scenarios are shown in Fig. 8. Blue blocks represent end-use heating technologies (hybrid HP-Bs) while red blocks represent district heating technologies (HNs). It is interesting to observe that all HNs are deployed in urban areas (the penetration of which is given in Table VIII) while only hybrid HP-B are applied in suburban, semirural and rural areas, demonstrating that heat density is the key driving/limiting factor for the application of HNs.

As shown in Fig. 8 (a), when integration is enabled, heating technology is shifted from hybrid HP-Bs to HNs. This drives larger investment in heat sector as can be derived from Fig. 5; capital investment in heat sector under integrated scenario are £3.54bn and £4.12bn larger under 100g/kWh and 50g/kWh respectively when compared with decoupled scenarios, due to the higher capital cost associated with district heating infrastructure (dominated by investments in HNs). On the other hand, large reduction in system operation costs and investment in NG CCS capacity, driven by enhanced system flexibility, drives considerable overall net savings. Overall, this analysis demonstrates that the integration of electricity and heat systems will drive increase in investment in heat infrastructure in order to reduce significantly operation and investment cost of the electricity system and ensure that the carbon target are met at the minimum whole-system cost.

In the light of Fig. 8 (b), the system integration also has a notable impact on the composition of annual heat production from different heating technologies. It can be observed that the integration increases heat production of NG CHP from 5% to 21%, under the carbon target of 100g/kWh. When the carbon target is 50g/kWh, increase in heat production of NG CHP is lower (from 0% to 7%), which is driven by the relatively high carbon intensity of NG CHP (CHP CCS is a potential low-carbon heat source, but according to the results of the simulation, it is not economic to deploy CHP CCS on a large scale based on the proposed carbon scenarios and the cost assumptions taken). Therefore, heat provided by IHPs increases from 0% to 21%, demonstrating that this technology may potentially play a significant role in decarbonizing heat (given its high COP) in the longer term.

E. Impact of Integration on Carbon Emissions

The integration of the electricity and heat system can influence the decarbonization strategies in different sectors. Table IX presents the optimized carbon intensities in electricity and heat sectors under given overall carbon targets. The carbon intensity of the heat sector represents CO2 emissions associated with total heat production (including electrified heat). Basically, the carbon emissions are driven by the conventional generation (e.g., CCGT, OCGT) on the electricity side and NG CHP together with gas boilers on the heat side.

TABLE IX
CARBON INTENSITY IN ELECTRICITY AND HEAT SECTOR

Overall carbon target (g/kWh)	System	Carbon intensity in electricity sector (g/kWh_{el})	Carbon intensity in heat sector (g/kWh_{th})
100	Integrated	124.6	77.9
	Decoupled	105.6	95.3
50	Integrated	55.8	43.4
	Decoupled	38.8	60.3

As shown in Table IX, the system integration increases the carbon intensity in the electricity sector and reduces the carbon emissions in the heat sector, while achieving the same overall carbon target. For the electricity sector, we observe from Fig. 6 (b) that when the integration is enabled, more electricity is generated by NG CHP, causing an overall increase in carbon emissions in the electricity sector. For the heat sector on the other hand, Fig. 8 (b) demonstrates that less gas-boiler-based heat and more electrified heat from HPs and NG CHPs (CHP is considered as a virtual HP [44]) is produced, thus reducing the carbon emissions in the heat sector.

As assumed in Section III-A, capacities of nuclear, wind and PV are specified, while NG CCS can be further added to the generation mix if the carbon targets cannot be satisfied. Therefore, the curtailment of VRE in the decoupled system is much higher than that in the integrated system, and hence more NG CCS is deployed to compensate the curtailment and meet the carbon target. On the one hand, although the curtailment of VRE is significantly alleviated through the system integration, the overall carbon intensity on the electricity side is still increased due to the significant reduction in generation from NG CCS. On the other hand, the system integration drives the electrification of the heat sector, thus reducing the carbon intensity on the heat side. The overall carbon intensities of both integrated system and decoupled system are the same. To summarize, higher carbon emissions in electricity sectors are allowed given lower carbon emissions in heat sectors, as the total carbon emissions are constant (meeting the same carbon target). This will lead to higher costs in heat sectors and lower costs in electricity sectors, but the overall system costs are reduced significantly.

This study indicates that the system integration can deliver the shift in carbon emissions from the heat sector to the electricity sector, driven by the shift in heat production from gas-boilers to NG CHPs while facilitating the electrification of the heat sector, which leads to significant cost savings in the electricity sector through the replacement of some NG CCS capacity by NG CHP (fundamentally enabled by the flexibility that significantly reduces VRE curtailment).

F. Value of TES

As TES plays an important role in facilitating the interaction between the electricity and the heat system, we specifically calculate the potential savings through the application of TES in the integrated electricity and heat system. In order to quantify the value of TES, we compare the costs of the integrated electricity and heat system with (main case) and without (counterfactual) TES. Table X summaries the annual savings in OPEX and CAPEX of the electricity sector and CAPEX of the heat sector through the application of TES under given carbon scenarios. Note that the CAPEX of TES for the main case is £0.78bn/year and £1.21bn/year under the carbon target of 100g/kWh and 50g/kWh respectively, while no TES is installed in the counterfactual.

TABLE X
SAVINGS FROM TES IN INTEGRATED ELECTRICITY AND HEAT SYSTEM

Carbon target (g/kWh)	OPEX (£bn/yr)	CAPEX of electricity Sector (£bn/yr)	CAPEX of heat sector (£bn/yr)	Total (£bn/yr)
100	1.84	0.78	-1.81	0.81
50	2.73	2.41	-3.10	2.05

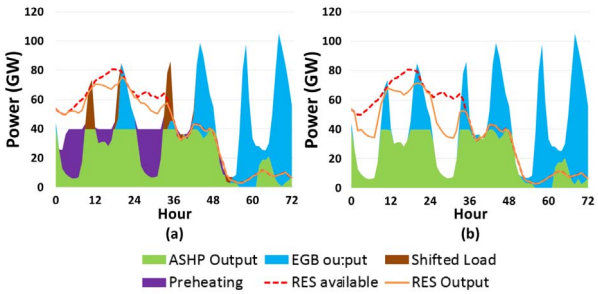

Fig. 9. Operating patterns of hybrid HP-Bs with (a) and without (b) preheating.

It can be seen that TES plays an important role in reducing the whole system operation and investment costs in the electricity sector at the cost of increasing the investment in the heat sector. Specifically, TES enables: a) delivery of operation savings through alleviating the curtailment of VRE, b) reduction of NG CCS capacity by supporting provision of ancillary services leading to an increase in VRE production and c) the shift in heat delivery from end-use to district based technologies, driven by the flexibility requirements (supported by the relatively low capital cost of industrial size TES).

G. Benefits From Pre-Heating

Due to the improved insulation of buildings, pre-heating through heat-driven electricity devices can enable further reduction in the operation cost of the integrated system although overall energy consumption increases. Fig. 9 illustrates the impact of preheating on the operation of hybrid HP-Bs spanning 3 days in winter. To highlight the impact of pre-heating, it is assumed in this case that all hybrid HP-B users participate in pre-heating. The results demonstrate that the level of pre-heating will be influenced by the amount of VRE production. Savings in the operation cost is achieved by shifting heat-load to the hours when VRE production is significant, which reduces VRE curtailment. On the other hand, during the hours when the availability of VRE is low, pre-heating is not extensively used. It should be noted that this analysis has been simplified by assuming that the flexibility enabled by preheating would not compromise the consumer comfort.

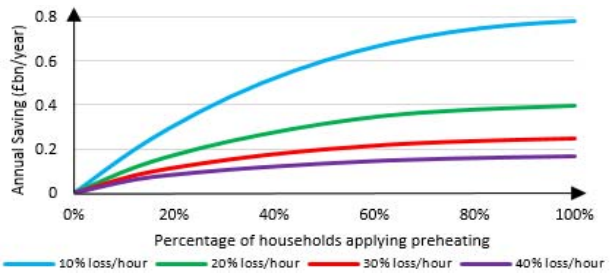

Fig. 10. Annual savings of the whole system through preheating.

TABLE XI
SAVINGS FROM THE INTEGRATION OF HEAT SYSTEM AND ELECTRICITY SYSTEM WITH INCREASED FLEXIBILITY

Carbon target (g/kWh)	OPEX (£bn/yr)	CAPEX of electricity sector (£bn/yr)	CAPEX of heat Sector (£bn/yr)	Total (£bn/yr)
100	1.24	0.66	-1.44	0.46
50	1.21	1.29	-1.34	1.15

The insulation levels of buildings as well as the percentage of households contributing to pre-heating are potential factors that may influence the value of pre-heating. In this context, Fig. 10 shows the annual savings associated with pre-heating considering (i) different insulation levels of buildings and (ii) different percentage of households participating in pre-heating. In addition to the savings in operation cost (driven by increased utilization of VRE), the application of pre-heating can also substitute a considerable amount of TES, driving further savings. From the results, it can be concluded that a) the value of pre-heating is intensely affected by the buildings insulation levels (energy efficiency); b) as expected, the marginal value of pre-heating declines with the increase of percentage of households providing this service.

H. Impact of Electricity Based Flexibility Measures

Significant potential savings can be achieved through the integration of the heat and electricity system according to Section III-B. However, the value of the integrated electricity and heat system may be significantly influenced by the availability of flexibility options in the electricity system. This section investigates the benefits through the integration of the heat system with a more flexible electricity system, compared to Section III-B, revealing the impact of the electricity-based flexibility measures on the value of the integration. For the illustrative purpose, this is carried out by enhancing the flexibility of the electricity system through (i) applying more efficient and more flexible thermal generation, (ii) adding 15GW of electrical energy storage that can provide all ancillary services and (iii) assuming that 20% of the non-heat driven electricity load is flexible to provide DSR. It should be stressed that the DSR constraints are only enabled in this case study.

The savings from the integration of the heat system and the electricity system with increased flexibility is given in Table XI. Compared with Section III-B, the total saving of the integrated electricity and heat system in this case reduces significantly, from £2.3bn/year to £0.46bn/year under the carbon target of 100g/kWh, and from £6bn/year to £1.15bn/year under the carbon target of 50g/kWh. This demonstrates that the benefits driven by the integration of the electricity and heat system may reduce accordingly if the flexibility within the electricity system increases. It is however important to note that the additional cost associated with enhancing the flexibility of the electricity system is not taken into account. To be specific, it is assumed that flexible thermal generators, electrical storage are already deployed in the electricity system while DSR can be dispatched without incurring any costs. In fact, it can be very capital-intensive to improve the flexibility of thermal generation and deploy electrical energy storage on a large scale. The potential cost that DSR can incur depends on consumers' willingness and behaviour which have significant uncertainty. Meanwhile, the heat system can provide substantial flexibility for the electricity system through system integration which otherwise will not be put into any use.

TABLE XII
LEVEL OF BALANCING SERVICES REQUIRED IN DIFFERENT SCENARIOS

	100g/kWh		50g/kWh	
	Reserve (GW)	Response (GW)	Reserve (GW)	Response (GW)
Maximum	9.8	5.9	14.9	9.3
Average	4.9	2.7	7.0	5.1

TABLE XIII
SAVINGS FROM SYSTEM INTEGRATION IN DIFFERENT SCENARIOS

		100g/kWh	50g/kWh
Savings from system integration (£billion/year)	Reserve and response considered	2.3	6
	No reserve and response requirement	0.8	2.2

I. Impact of Balancing Service Requirements on the Value of System Integration

The level of balancing services required has a significant impact on the value of system integration. The average and maximum amounts of reserve and response services in different scenarios are presented in Table XII, that correspond to the generation scenarios presented in Fig. 6 (a). It can be observed that reduction in carbon emissions significantly increases the amount of balancing services.

Table XIII presents the cost savings associated with system integration under two carbon targets in two cases. In the first case, the volumes of reserve and response required are modeled as described in Section III-B, while in the second case, the assumption is made that no balancing services would be required. It can be observed that the benefits of system integration significantly decrease when there is no need for the provision of balancing services. Moreover, as expected, the benefits of system integration are larger under the lower carbon target.

IV. CONCLUSION

This paper proposes a novel whole-system investment model for the optimization of integrated electricity and heat

systems, simultaneously considering operation and investment time horizons at both local and national level. This model is applied to optimize the decarbonization strategies of combined electricity and heat systems, while assessing the values of the integration of electricity and heat system and revealing trade-offs between electrification of heat sector through HNs and through electrified heat at the consumer end side.

A series of case studies are carried out to quantify the benefits driven by the integration of the electricity and heat systems based on the cost assumptions. The analysis demonstrated that increased investment in district heating infrastructure will enhance system flexibility that will in turn deliver larger cost savings in the operation and investment of the electricity system, ensuring that the carbon target is met at the minimum whole-system cost. Furthermore, the benefits of the application of TES, preheating and enhancing the flexibility of the electricity system, on the value of the system integration are also quantified. Additionally, the analysis also demonstrates that the level of balancing service requirements would have a major impact on the value of the system integration. In this context, provision of balancing services by different technologies, including the contribution of VRE, nuclear generation, emerging flexibility technologies, etc., would potentially have a considerable impact on the value of the system integration.

It will be important to further enhance the model by investigating the significance of the strategic investment, particularly in the heat infrastructure and the potential role and value of hydrogen technologies. It is also significant to consider the importance of the transport sector in the integrated energy system and develop more detailed understanding of the impact of building efficiency and HNs. In this context, further work is required to understand the impact of preheating on the consumer comfort. In order to identify robust strategies for the decarbonization of the integrated electricity and heat sectors, it is essential to understand the impact of considerable uncertainties in future cost of different technologies. Furthermore, more advanced methods for the selection of representative days to further enhance the efficiency of calculation without compromising the accuracy should be investigated.

REFERENCES

[1] R. Sansom and G. Strbac, "The impact of future heat demand pathways on the economics of low carbon heating systems," in *Proc. BIEE 9th Acad. Conf.*, 2012, pp. 19–20.

[2] E. Lannoye, D. Flynn, and M. O'Malley, "Evaluation of power system flexibility," *IEEE Trans. Power Syst.*, vol. 27, no. 2, pp. 922–931, May 2012.

[3] G. Strbac *et al.*, *Value of Flexibility in a Decarbonised Grid and System Externalities of Low-Carbon Generation Technologies*, Imperial College London, London, U.K., and NERA Econ. Consult., White Plains, NY, USA, 2015.

[4] G. Strbac *et al.*, *Understanding the Balancing Challenge*, Dept. Energy Climate Change, London, U.K., Aug. 2012.

[5] P. Mancarella and G. Chicco, "Integrated energy and ancillary services provision in multi-energy systems," in *Proc. IREP Symp. Bulk Power Syst. Dyn. Control IX Optim. Security Control Emerg. Power Grid*, 2013, pp. 1-19.

[6] X. Chen *et al.*, "Increasing the flexibility of combined heat and power for wind power integration in China: Modeling and implications," *IEEE Trans. Power Syst.*, vol. 30, no. 4, pp. 1848–1857, Jul. 2015.

[7] J. Kiviluoma and P. Meibom, "Influence of wind power, plug-in electric vehicles, and heat storages on power system investments," *Energy*, vol. 35, no. 3, pp. 1244–1255, 2010.

[8] G. Li *et al.*, "Optimal dispatch strategy for integrated energy systems with CCHP and wind power," *Appl. Energy*, vol. 192, pp. 408–419, Apr. 2017.

[9] H. Lund, B. Möller, B. V. Mathiesen, and A. Dyrelund, "The role of district heating in future renewable energy systems," *Energy*, vol. 35, no. 3, pp. 1381–1390, 2010.

[10] F. Fang, Q. H. Wang, and Y. Shi, "A novel optimal operational strategy for the CCHP system based on two operating modes," *IEEE Trans. Power Syst.*, vol. 27, no. 2, pp. 1032–1041, May 2012.

[11] D. D. Andrews *et al.*, *Background Report on EU-27 District Heating and Cooling Potentials, Barriers, Best Practice and Measures of Promotion*, Publications Office Eur. Union, Luxembourg City, Luxembourg, 2012.

[12] *Heat Pumps in District Heating*, DECC, London. U.K., 2016. [Online]. Available: https://www.gov.uk/government/publications/heat-pumps-in-district-heating

[13] M. B. Blarke and H. Lund, "Large-scale heat pumps in sustainable energy systems: System and project perspectives," *Thermal Sci.*, vol. 11, no. 3, pp. 143–152, 2007.

[14] P. Mancarella, "Cogeneration systems with electric heat pumps: Energy-shifting properties and equivalent plant modelling," *Energy Convers. Manag.*, vol. 50, no. 8, pp. 1991–1999, 2009.

[15] K. Hedegaard, B. V. Mathiesen, H. Lund, and P. Heiselberg, "Wind power integration using individual heat pumps—Analysis of different heat storage options," *Energy*, vol. 47, no. 1, pp. 284–293, 2012.

[16] K. Hedegaard and M. Münster, "Influence of individual heat pumps on wind power integration—Energy system investments and operation," *Energy Convers. Manag.*, vol. 75, pp. 673–684, Nov. 2013.

[17] P. Mancarella, "MES (multi-energy systems): An overview of concepts and evaluation models," *Energy*, vol. 65, pp. 1–17, Feb. 2014.

[18] S. Heinen, D. Burke, and M. O'Malley, "Electricity, gas, heat integration via residential hybrid heating technologies—An investment model assessment," *Energy*, vol. 109, pp. 906–919, Aug. 2016.

[19] S. Heinen and M. O'Malley, "Power system planning benefits of hybrid heating technologies," in *Proc. IEEE Eindhoven PowerTech*, 2015, pp. 1–6.

[20] K. Klein, K. Huchtemann, and D. Müller, "Numerical study on hybrid heat pump systems in existing buildings," *Energy Build.*, vol. 69, pp. 193–201, Feb. 2014.

[21] Z. Pan, Q. Guo, and H. Sun, "Feasible region method based integrated heat and electricity dispatch considering building thermal inertia," *Appl. Energy*, vol. 192, pp. 395–407, Apr. 2017.

[22] Z. Li, W. Wu, M. Shahidehpour, J. Wang, and B. Zhang, "Combined heat and power dispatch considering pipeline energy storage of district heating network," *IEEE Trans. Sustain. Energy*, vol. 7, no. 1, pp. 12–22, Jan. 2016.

[23] C. Lin, W. Wu, B. Zhang, and Y. Sun, "Decentralized solution for combined heat and power dispatch through benders decomposition," *IEEE Trans. Sustain. Energy*, vol. 8, no. 4, pp. 1361–1372, Oct. 2017.

[24] A. Hast, S. Rinne, S. Syri, and J. Kiviluoma, "The role of heat storages in facilitating the adaptation of district heating systems to large amount of variable renewable electricity," *Energy*, vol. 137, pp. 775–788, Oct. 2017.

[25] X. Liu and P. Mancarella, "Modelling, assessment and Sankey diagrams of integrated electricity-heat-gas networks in multi-vector district energy systems," *Appl. Energy*, vol. 167, pp. 336–352, Apr. 2016.

[26] A. Ahmed and P. Mancarella, "Strategic techno-economic assessment of heat network options for distributed energy systems in the U.K.," *Energy*, vol. 75, pp. 182–193, Oct. 2014.

[27] C. Bordin, A. Gordini, and D. Vigo, "An optimization approach for district heating strategic network design," *Eur. J. Oper. Res.*, vol. 252, no. 1, pp. 296–307, 2016.

[28] D. Pudjianto, M. Aunedi, P. Djapic, and G. Strbac, "Whole-systems assessment of the value of energy storage in low-carbon electricity systems," *IEEE Trans. Smart Grid*, vol. 5, no. 2, pp. 1098–1109, Mar. 2014.

[29] M. Carrion and J. M. Arroyo, "A computationally efficient mixed-integer linear formulation for the thermal unit commitment problem," *IEEE Trans. Power Syst.*, vol. 21, no. 3, pp. 1371–1378, Aug. 2006.

[30] F. Teng, V. Trovato, and G. Strbac, "Stochastic scheduling with inertia-dependent fast frequency response requirements," *IEEE Trans. Power Syst.*, vol. 31, no. 2, pp. 1557–1566, Mar. 2016.

[31] F. Teng and G. Strbac, "Full stochastic scheduling for low-carbon electricity systems," *IEEE Trans. Autom. Sci. Eng.*, vol. 14, no. 2, pp. 461–470, Apr. 2017.
[32] J. P. Green, S. A. Smith, and G. Strbac, "Evaluation of electricity distribution system design strategies," *IEE Proc. Gener. Transm. Distrib.*, vol. 146, no. 1, pp. 53–60, Jan. 1999.
[33] G. Strbac *et al.*, *Strategic Assessment of the Role and Value of Energy Storage Systems in the U.K. Low Carbon Energy Future*, Carbon Trust, London, U.K., 2012.
[34] DECC. *National Heat Map*. Accessed: Mar. 5, 2017. [Online]. Available: http://nationalheatmap.cse.org.uk/
[35] C. K. Gan, P. Mancarella, D. Pudjianto, and G. Strbac, "Statistical appraisal of economic design strategies of LV distribution networks," *Elect. Power Syst. Res.*, vol. 81, no. 7, pp. 1363–1372, 2011.
[36] *Electricity Generation Costs*, BEIS, London, U.K., Nov. 2016. [Online]. Available: https://www.gov.uk/government/publications/beis-electricity-generation-costs-november-2016
[37] *Technology Data for Energy Plants—Generation of Electricity and District Heating, Energy Storage and Energy Carrier Generation and Conversion*, Energi Styrelsen, Copenhagen, Denmark, 2012.
[38] *Assessment of the Costs, Performance, and Characteristics of U.K. Heat Networks*, DECC, London, U.K., 2015. [Online]. Available: https://www.gov.uk/government/publications/assessment-of-the-costs-performance-and-characteristics-of-uk-heat-networks
[39] R. Abdurafikov *et al.*, "An analysis of heating energy scenarios of a finnish case district," *Sustain. Cities Soc.*, vol. 32, pp. 56–66, Jul. 2017.
[40] J. Ma, V. Silva, R. Belhomme, D. S. Kirschen, and L. F. Ochoa, "Evaluating and planning flexibility in sustainable power systems," *IEEE Trans. Sustain. Energy*, vol. 4, no. 1, pp. 200–209, Jan. 2013.
[41] K. Poncelet, H. Höschle, E. Delarue, A. Virag, and W. D'haeseleer, "Selecting representative days for capturing the implications of integrating intermittent renewables in generation expansion planning problems," *IEEE Trans. Power Syst.*, vol. 32, no. 3, pp. 1936–1948, May 2017.
[42] M. Sun, F. Teng, I. Konstantelos, and G. Strbac, "An objective-based scenario selection method for transmission network expansion planning with multivariate stochasticity in load and renewable energy sources," *Energy*, vol. 145, pp. 871–885, Feb. 2018.
[43] F. Teng and G. Strbac, "Assessment of the role and value of frequency response support from wind plants," *IEEE Trans. Sustain. Energy*, vol. 7, no. 2, pp. 586–595, Apr. 2016.
[44] R. Lowe, "Combined heat and power considered as a virtual steam cycle heat pump," *Energy Policy*, vol. 39, no. 9, pp. 5528–5534, 2011.

Xi Zhang (S'17) received the bachelor's and master's degrees in electrical engineering from Tsinghua University, Beijing, China, in 2012 and 2014, respectively. He is currently pursuing the Ph.D. degree with Imperial College London, London, U.K. His research interests include whole-energy system planning and multivector energy system modeling.

Goran Strbac (M'95) is currently a Professor of energy systems with Imperial College London, London, U.K. His research interests include modeling and optimization of economics and security of energy system operation and investment, energy infrastructure reliability, and future energy markets, including integration of emerging technologies in supporting cost-effective evolution to smart low carbon energy future.

Nilay Shah is currently a Professor and the Head of the Department of Chemical Engineering with Imperial College London, London, U.K. His research interests include design and analysis of energy systems, supply chain design and optimization, process synthesis and development for fine chemicals, pharmaceutical and biochemical processes, and safety in design and operation, especially the application of formal mathematical techniques to assess, and improve process safety.

Fei Teng (M'15) received the bachelor's degree in electrical engineering from Beihang University, Beijing, China, in 2009 and the Ph.D. degree in electrical engineering from Imperial College London, London, U.K., in 2015. He is currently a Lecturer with Control and Power Group, Imperial College London. His research interests include power system control and operation, system flexibility, and stochastic optimization.

Danny Pudjianto (M'98) received the B.Sc. degree in electronics from Institut Teknologi Sepuluh Nopember, Surabaya, Indonesia, in 1996, and the master's and Ph.D. degrees in power system engineering from the University of Manchester Institute of Science and Technology, Manchester, U.K., in 1999 and 2003, respectively. He is currently a Research Fellow with Imperial College London.